Proceedings World Geothermal Congress 2020+1
Reykjavik, Iceland, April - October 2021

A High Performance Framework for the Optimization of Geothermal Systems, Comparing Energy Production and Economic Output

Alexandros Daniilidis[a], Mark Khait[a], Sanaz Saeid[a], David F. Bruhn[a,b] and Denis Voskov[a,c]

[a] Delft University of Technology, Stevinweg 1, 2628 CN Delft, Netherlands

[b] Helmholtz Center Potsdam GFZ, Germany.

[c] Stanford University, CA 94305-4007, USA.

a.daniilidis@tudelft.nl, D.V.Voskov@tudelft.nl

Keywords: optimization, resource assessment, economics, direct-use, hydraulic thermal, development, regulation

ABSTRACT

Geothermal heat production for direct use often faces economic challenges that might hinder its more widespread deployment. Design and operation choices in geothermal field development require the evaluation of a multitude of factors with different levels of uncertainty. Energy production and economic output of geothermal systems can therefore be very sensitive to well production rates and reservoir properties such as permeability, while regulatory constraints could further increase complexity. In this work, a high performance framework for optimization of geothermal systems is developed using the Delft Advanced Research Terra Simulator (DARTS) and the Sequential Least Squares Programming (SLSQP) optimization algorithm. An optimization is performed in a system with two doublets by changing the rates of each doublet separately every year, over a thirty year period. Two different objective functions are optimized for: energy generation and NPV. With the maximum injection constraint active both objective functions arrive to almost identical solutions, while removing the constraint improved both the energy generation and NPV only for the NPV objective function. The framework achieved an average convergence time below 5 hours for the full optimization cycle and an average simulation runtime just below 10 seconds. This analysis suggest that the NPV is a better suited optimization function than the energy generation as it encompasses more system aspects. The high performance of the optimization framework will prove increasingly important as more uncertainties are considered in the optimization process.

1. INTRODUCTION

The trade-off between geothermal field lifetime and economic output is highly pertinent, especially for low-enthalpy, direct-use geothermal systems. Such systems exhibit low profit margins and long break even times (Daniilidis et al., 2017a), which might hinder their widespread development. Developers therefore could aim for intensifying exploitation by utilizing higher production rates, as this can improve their business case (Daniilidis et al., 2020). Intensified exploitation could lead to shorter system lifetimes and increased interference between adjacent systems (Cees J.L. Willems et al., 2017b). Different optimization strategies are likely to arise from the perspective of a developer aiming to improve economic output and a regulator aiming for the long term energy contribution or a larger number of systems overall.

Well spacing and system lifetime have been shown to have a linear relation in homogenous systems (Saeid et al., 2015). However, reducing the well spacing allows for more doublets to be positioned within a given area (C. J. L. Willems et al., 2017; Willems and M. Nick, 2019); this results in more energy being produced and is therefore important for regional geothermal development and a larger contribution of geothermal energy to the greater energy supply.

Previous studies have shown a more sustainable geothermal resource utilization using seasonally adjusted rates (Daniilidis et al., 2017b), implying that system lifetime can be extended if geothermal energy production is dictated by heat demand. This however might have operational implications and therefore flow rate changes over larger time periods might be preferable.

Regional level studies have often considered homogeneous reservoir properties for simplicity (Willems and M. Nick, 2019). Nonetheless, depending on effective permeability encountered by the wells and possible interference between systems, pressure levels might not allow for uniform injection-production rates over a great area. Considering the regulatory framework that constrains the maximum injected pressures (SodM and TNO-AGE, 2013) it is therefore crucial to consider these constraints for a realistic resource assessment.

Recently, the importance of an integrated simulation framework that can be easily adapted to evolving computing architectures has been showcased (Khait and Voskov, 2019). This framework, named the Delft Advanced Research Terra Simulator (DARTS) (DARTS, 2019) enables a computationally efficient, forward problem solution based on the Operator Based Linearization approach (Khait and Voskov, 2018; Voskov, 2017). Benchmarked with other prominent simulators DARTS was found to be highly efficient while maintaining high levels of accuracy (Wang et al., 2019).

Optimization efforts for hydrocarbon reservoirs have shown the importance of rate control in defining optimal production strategies with respect to improving the generated NPV (Barros et al., 2019; Chen et al., 2017; Fonseca et al., 2014; van Essen et al., 2009). Optimization studies for geothermal systems have focused on doublet positioning within a 3D heterogeneous reservoir (Akin et al., 2010) and additional optimization of the NPV (Kahrobaei et al., 2019). Other studies considering the economic performance, where limited to 2D models (Kong et al., 2017). A comparison between optimization on different objective functions in a 3D heterogeneous reservoir is currently lacking in scientific literature.

In this work a high performance framework for optimization is developed, based on the DARTS simulator and utilizing the Sequential Least Squares Programming method (SLSQP). The controls available to the optimizer are the rates of each doublet on a yearly basis over a period of 30 years. The framework is used to optimize two objective functions, namely the cumulative produced energy and the generated NPV.

2. MODEL

2.1 Reservoir model

A Thermal-Hydraulic (TH) model is used as the basis for the simulations. The model parameters are based on previously published work (Cees J.L. Willems et al., 2017a) on the channelized system of the Delft Sandstone member (DSSM), situated at the West Netherlands Basin. The 3D model has dimensions of 1800 m by 1200 m by 105 m (x,y,z), is comprised of circa 100k cells (60 x 40 x 42), and its properties are derived from a finer resolution model using the geometric upscaling of properties. The top and bottom layers act as infinitely large domains with fixed temperature, providing conductive thermal recharge to the reservoir layers. A detailed documentation of the used model has been previously published in Shetty et al. (2018) and Wang et al. (2019).

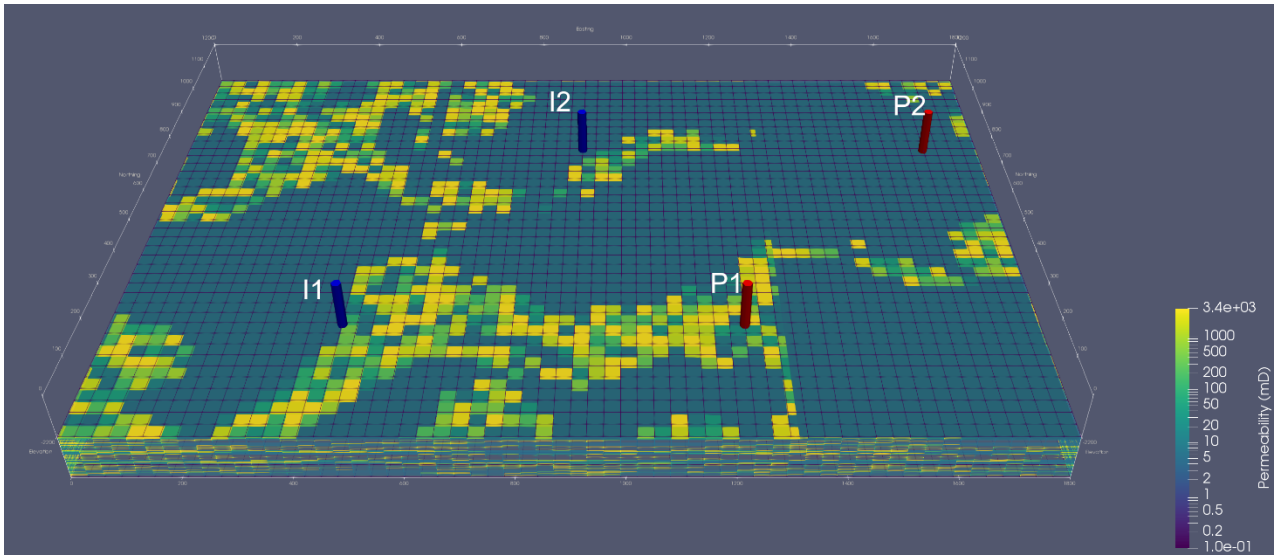

Figure 1. Angled overview of the reservoir model showing the positioning of the wells. Each cells is 30 m by 30 m by 2.5 m (x,y,z).

In this model, two doublets are positioned with a well spacing of 780 m along the main axis of the model (E-W). The location of the wells is chosen arbitrarily. The injection and production wells have the same orientation, with the second doublet axis being offset 450 m towards the west and spaced about 600 m away from the first doublet axis (Figure 1). The injection temperature is 30 °C.

2.2 Energy production and NPV

The produced power (W) at the wells, used for the calculation of income is computed according to:

$$P_{well} = Q\rho_f\, c_f\, \Delta T \tag{1}$$

in which Q is the flow rate (m^3/s) and ΔT is the temperature difference between producer and injector wells (K). The required pump power (W) only considers the pressure drop in the reservoir:

$$P_{pump} = \frac{\Delta P \cdot Q}{\eta} \tag{2}$$

where ΔP is the pressure difference between the wells (Pa), Q is the flow rate (m^3/s) and η is the pump efficiency. The overall system power is then calculated as:

$$P_{system} = P_{well} - P_{pump} \tag{3}$$

Cumulative energy generated by the system is computed according to:

$$E_{cum} = \sum_{t=0}^{n} P_{well_t} \tag{4}$$

where n is the project years and t the time. The cost of drilling the wells (€) is computed according to (TNO, 2018):

$$C_{well} = 375000 + 1150Z \quad + 0.3Z^2 \tag{5}$$

where Z is the measured depth alonghole. The NPV is calculated similarly to Daniilidis et al., (2017a) as:

$$NPV = \sum_{t=0}^{n} \frac{CF_t}{(1+r)^t} \quad (6)$$

where CF is the cashflow, r the discount rate, n is the project years and t the time. The cumulative produced power generated income based on the heat price, while the pump power costs are computed based on the electricity price. The inputs considered for the power production and NPV calculation are summarized in Table 1. In order to evaluate the combined system the generated energy is first calculated on a doublet basis. The aggregated results are then used for the NPV calculations, over 100 day intervals. Two objective functions are considered for the optimization, namely the cumulative energy produced (eq. 5) and the NPV (eq 7).

Table 1. Energy generation and NPV inputs

Load factor (%)	Heat price (€/MWh)	Pump cost (k€)	Pump lifetime (yrs)	Pump efficiency (%)	OpEx % of CapEx (%)	Discount rate (%)	Electricity price (€/MWh)
90	60	500	5	60	5	5	100

2.3 Bottom Hole Pressure limit and penalty

The bottom hole pressure of the model is taking into account the SodM directive for injection pressure in geothermal energy systems (SodM and TNO-AGE, 2013). This is implemented by penalizing the energy production proportionally to the rate of exceedance over the SodM threshold. The implementation of the maximum injection pressure is derived as follows:

$$BHP_{max} = 0.0135 Rtop_{TVD} \quad (7)$$

where $Rtop_{TVD}$ is the True Vertical Depth (TVD) of the reservoir top that the well encounters. When the maximum injection pressure is exceeded, the system power is reduced by the overpressure above BHP_{max} multiplied by a penalty factor of 10. This is necessary to create an increasing reduction of the produced energy and therefore steer the optimizer to maintain the production rates below this threshold. At any point, both injection and producer wells of a single doublet have the same flow rates.

2.4 Optimizer setup

The optimizer used is the Sequential Least Squares Programming method (SLSQP) as implemented in SciPy (Jones et al., 2001), that also makes use of the NumPy library (Oliphant, 2006). It is a local constrained gradient-based optimization algorithm. This implementation of the SLSQP algorithm has been successfully used in other engineering contexts and proved efficient in finding the minimum of an objective function with up to hundreds of unknowns (i.e. optimization parameters) (Wendorff et al., 2016). In order to ensure that local minimums, found by the optimizer, represent the global minimum, four different initial guesses are used for each optimization. The optimizer is allowed to alter the rates on yearly basis, independently for each doublet, while the wells in each doublet have the same rate at all times. The minimum and maximum rates available to the optimizer are 0.042 m^3/h and 625 m^3/h respectively. Additionally, the solution tolerance is also altered to ensure consistency of the converged solution. Finally, to show the effect of the BHP limit the BHP penalty is also removed. These inputs are shown in Table 2.

Table 2. Optimizer input and controls

	Tolerance	Initial guess	BHP penalty	Rate constraints	Maximum iterations
Values	1e-2, 1e-3	Uniform 4.2 m3/h, Uniform 300.0 m3/h, Uniform 500.0 m3/h, random	10, Off	min: 0.042 m^3/h max: 625 m^3/h	100

2.5 Evaluation of objective function and its gradient

The SLSQP is a gradient-base iterative optimization method. It requires frequent evaluation of the objective function (several per iteration) and its gradient (once per iteration). Each evaluation of the objective function requires a single forward simulation; each gradient evaluation involves 60 forward simulations (one for each of the optimization parameters – yearly rates for each of the two doublets over a 30 year period). Therefore, forward simulations occupy more than 99% of the overall optimization time, hence simulation performance is imperative for the efficiency of the optimization framework.

While DARTS already provides very competitive geothermal simulation performance in single-threaded mode, it is possible to improve it further using parallel hardware architectures. Each optimization was performed on a dedicated cluster node equipped by two Intel Xeon CPU E5-2650 v3 processors with 10 physical cores each. For the objective function evaluation, a multithreaded mode was enabled with 20 threads. This allowed to decrease simulation time for the objective function evaluation by a factor of 3.

The gradient evaluation is more critical, since it involves even more forward simulations. Fortunately, these computations are embarrassingly parallel: all of forward runs are completely independent and can be performed simultaneously, each in a separate process. The optimal amount of processes was found experimentally and matched the number of cores of available cores (20). Hence, 60 simulations were performed in three batches, 20 simulations each. In this case, a single-threaded DARTS mode was used. This allowed to decrease simulation time in the gradient evaluation by a factor of 11.

3. RESULTS

3.1 Optimization results

3.1.1. Energy production

Optimization of the cumulative produced energy function from an initial guess of 500 m3/h and with the BHP penalty active, the cumulative produced energy exhibits negative values (Figure 2). This is due to the fact that the BHP penalty is activated and the energy production is penalized, since the maximum BHP is exceeded. The optimizer then responds by first decreasing the rates substantially, which leads to positive but very low values of produced cumulative energy. In the following iterations, the rates are gradually increased for both doublets until the maximum rates are found that remain below the maximum allowed BHP and do not activate the penalty. The converged solution achieves a maximum produced cumulative energy of circa 5 TWh after 30 years, while the NPV achieved is circa 25 M€. Compared to the initial guess value, the production temperature of both doublets drops less, since the converged solution results in lower flow rates. The fact that the converged solution results in different rates for each production well implies that the two respective injection wells encounter different permeability in the reservoir: the first well (I1) encounters higher permeability and is able to use increased flow rates for the same BHP pressure, while the opposite is true for the second well (I2). Since well in each doublet always have the same flow rates, the injection rates that stay below the BHP limit are also applied as production rates to the respective production wells.

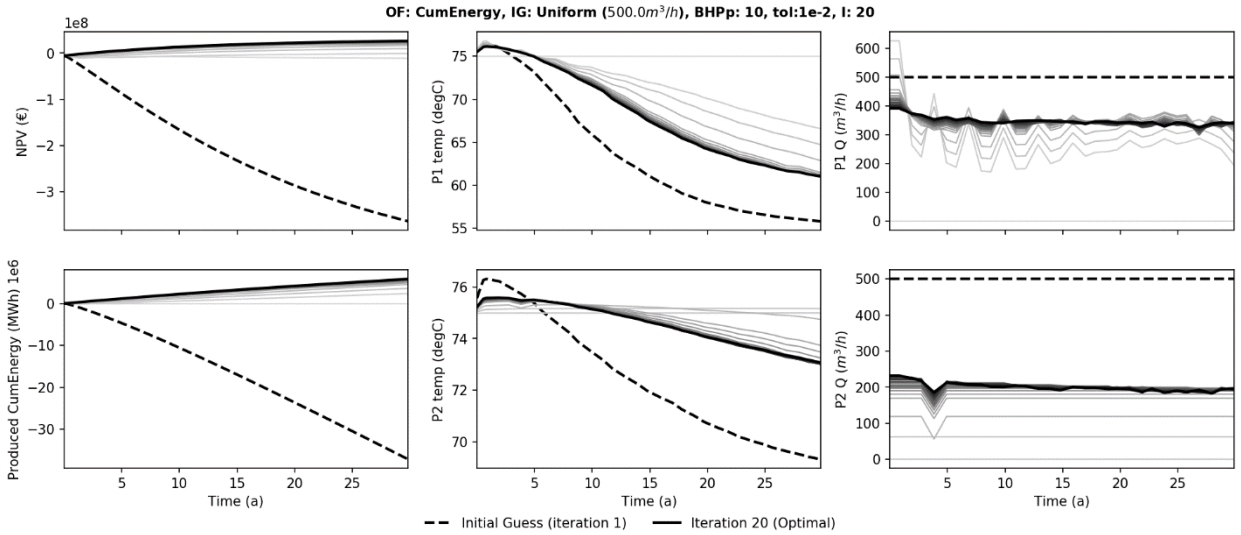

Figure 2. Optimization on the objective function (OF) cumulative energy production using a uniform initial guess (IG) of 500 m^3/h, with an active BHP penalty (BHPp) of 10 and a solution tolerance (tol) of 1e-2. The optimal solution required 20 iterations (I).

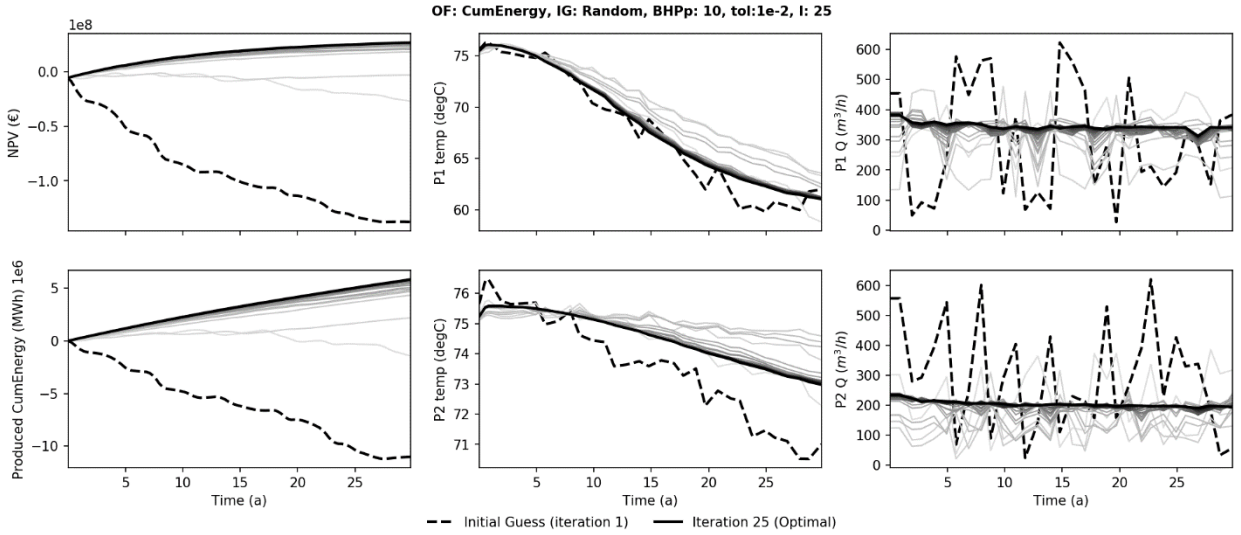

Figure 3. Optimization on the objective function (OF) cumulative energy production using a random initial guess (IG), with an active BHP penalty (BHPp) of 10 and a solution tolerance (tol) of 1e-2. The optimal solution required 25 iterations (I).

With a random initial guess for both wells and the BHP penalty active, the cumulative produced energy as well as the NPV exhibit again negative values (Figure 3). Some of the random rates used results in a BHP that exceeds the maximum BHP allowed and activate the penalty. Nonetheless, the optimization converges again to very similar values as for the uniform initial guess of

500m^3/h (Figure 2). The converged solution rates of both wells are circa 400 m^3/h for P1 and circa 240 m^3/h for P2 and decline slightly over time.

The overview of the converged solutions using the optimization function cumulative produced energy and all the optimizer inputs and controls as shown in Table 2, is presented in Figure 4. A very good agreement of the curves of cumulative produced energy, NPV and production temperature curves for both well can be observed for all converged solution with an active BHP penalty. The well rates exhibit slight variations, which could be attributed to multiple solutions leading to the same cumulative produced energy, NPV and temperature results. Nonetheless, the overall pattern is consistent and values are quite close. The converged solutions for both a uniform and a random initial guess with the BHP penalty are in perfect agreement. Removing the BHP penalty, results in both wells using the highest rates available to the optimizer (625 m^3/h – see also 2.4 Optimizer setup), resulting in even higher values of produced cumulative energy but with decreased NPV, and production temperatures for both wells.

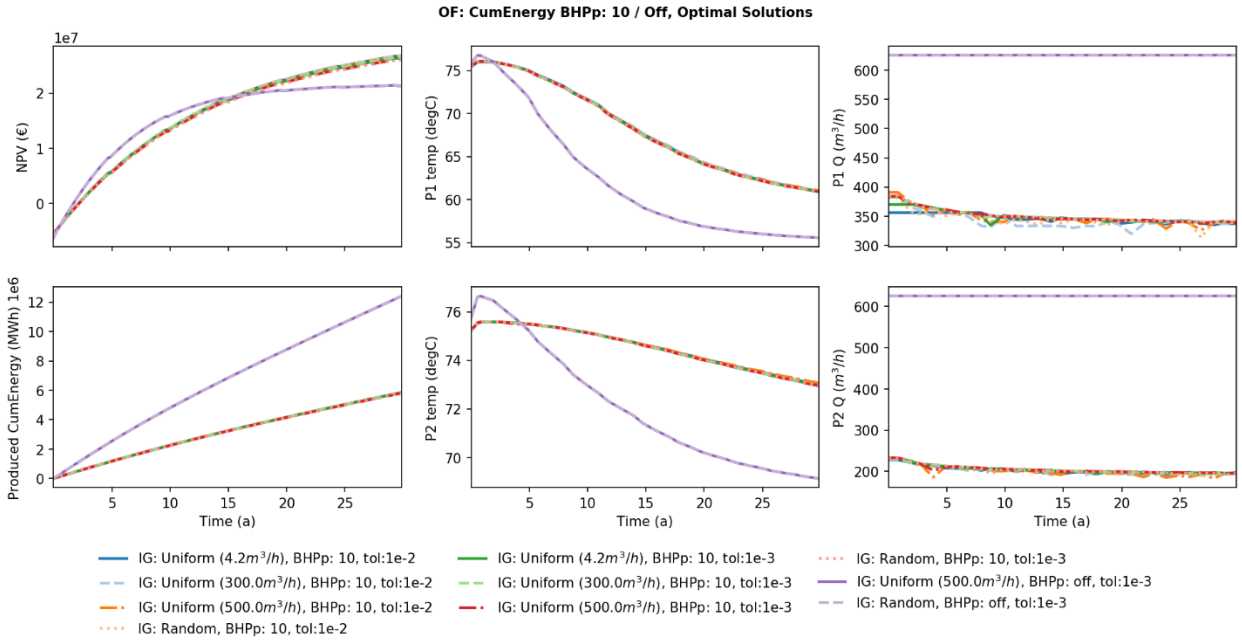

Figure 4. All converged solutions for the optimized Energy objective function (OF) for the different initial guess (IG), BHP penalty (BHPp), solution tolerance (tol).

3.1.2. NPV

Starting from the lowest initial guess of 4.2 m^3/h when optimizing the NPV function results in negative NPV values (Figure 5). The optimizer then gradually increases the rates of both wells until the injection rates of the wells reach the BHP limit value. Similarly, starting from a random initial guess, we observe that both well converge to the same rates of about 340 m^3/h for the first doublet and 230 m3/h for the second doublet (Figure 6). The resulting NPV value is also matching at 25M€.

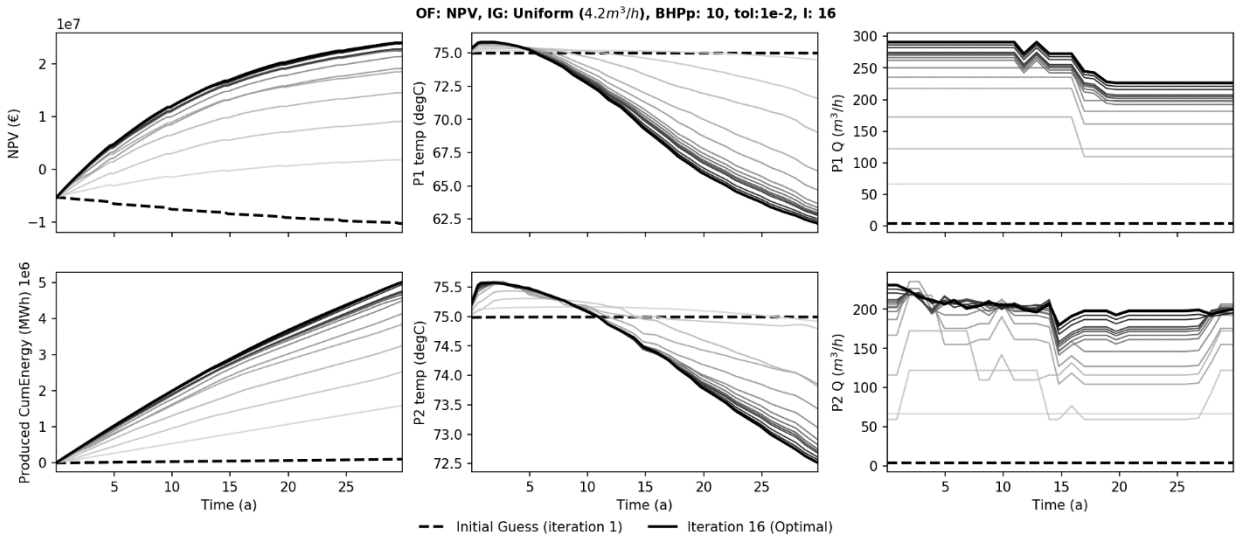

Figure 5. Optimization on the objective function (OF) NPV using a uniform initial guess (IG) of 4.2m^3/h, with a n active BHP penalty (BHPp) of 10 and a solution tolerance (tol) of 1e-3. The optimal solution required 16 iterations (I).

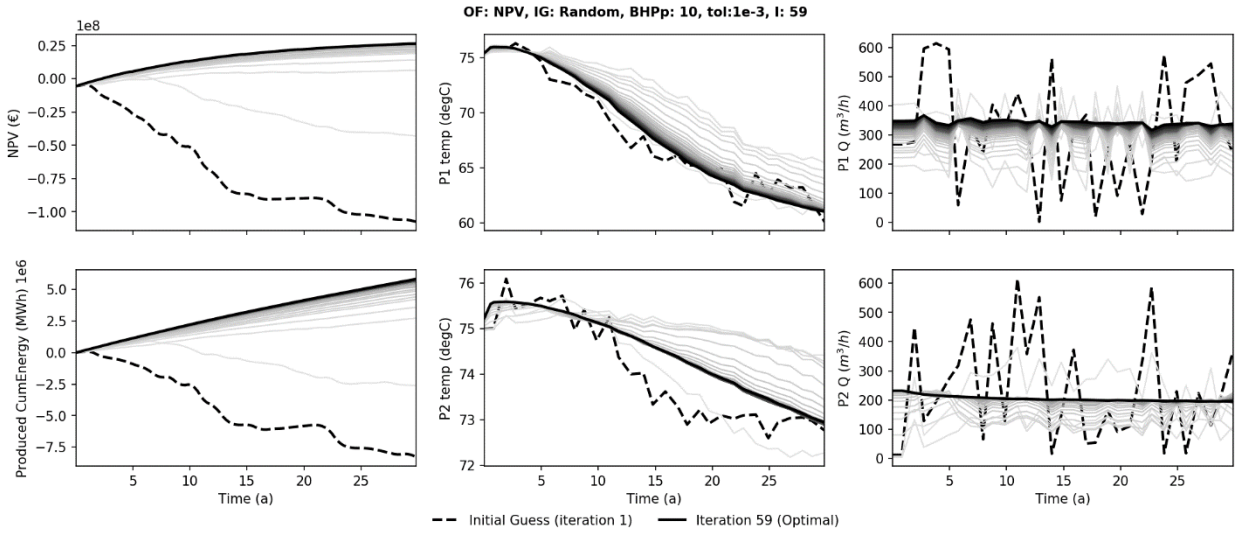

Figure 6. Optimization on the objective function (OF) NPV using a random initial guess (IG), with a n active BHP penalty (BHPp) of 10 and a solution tolerance (tol) of 1e-3. The optimal solution required 59 iterations (I).

A comparing of the converged solutions using the optimization function NPV and all the optimizer inputs and controls as shown in Table 2, is presented in Figure 7. The NPV curves show a close match but there is a range between 24 and 26 M€ for the solutions where the BHP limit is activated. The respective cumulative produced energy also exhibits a range between 5 TWh and 5.8 TWh. Similarly, the production temperature curves show a variation of circa 0.7 °C for the first production well (P1) and circa 0.5 °C for the second production well (P2). The rates of doublet 1 show great variability with differences of up to 100 m3/h even though the shape of the curves is consistent with higher rates in the first years that are reduced towards the last years. Contrary to this, the rates of the second doublet are more consistent. Removing the BHP penalty results in an NPV value of 32.5 M€. This is achieved with significantly higher rates in the first years for the first doublet to increase production and revenues, that is drastically lowered towards the last years. Lowering the rates so drastically implies that the optimizer tries to postpone thermal breakthrough for the first doublet. The second doublet also uses higher flow rates in the first years but the reduction is not so strong towards the last years. The slight increase of the rates in the last five years suggest that the production temperature of the second doublet is higher. Indeed the temperature curves of the production wells corroborate this; the production temperature of the first doublet drops below 60 °C, while for the second doublet it only drops to circa 71 °C.

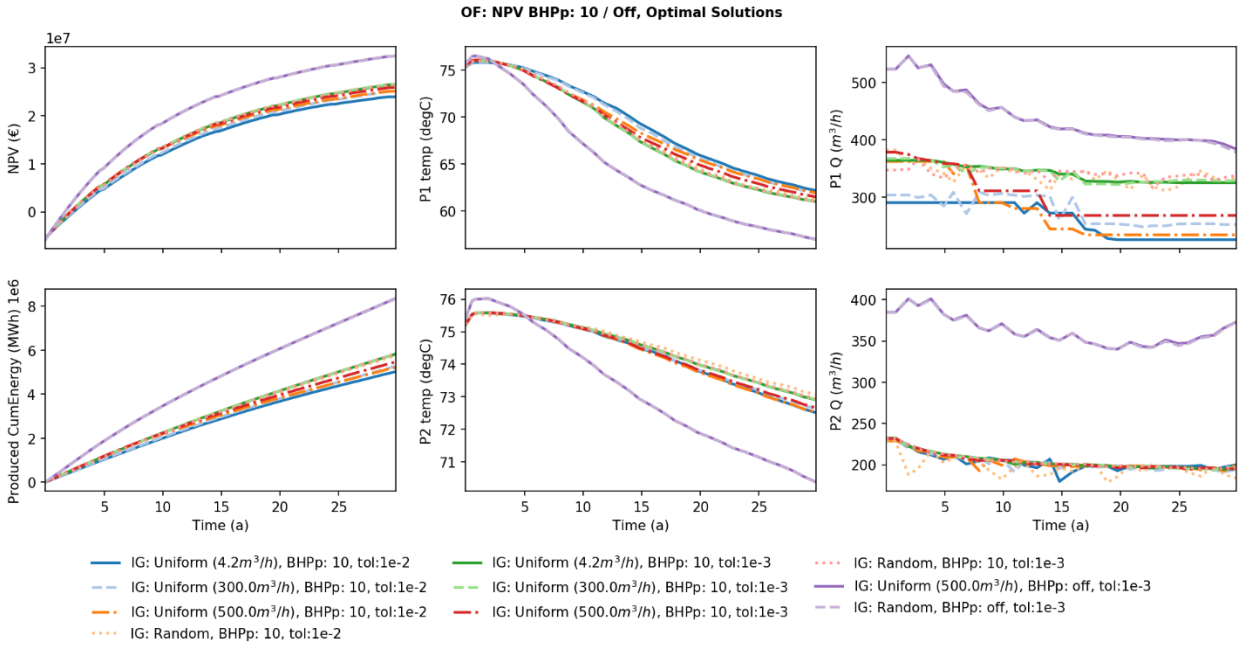

Figure 7. All converged solutions for the optimized NPV objective function (OF) for the different initial guess (IG), BHP penalty (BHPp), solution tolerance (tol).

3.1.3. Comparison of the optimal solutions for Cumulative Energy and NPV objective functions

The optimization of the objective functions of NPV and cumulative energy produced converged to almost identical results when the BHP penalty was active(Figure 8). Some slight deviations in the rates of the first doublet can still be observed. Nonetheless, the NPV and cumulative energy produced curves show a very good match, regardless of the objective function used. When the BHP

penalty is removed, the converged solution exhibit different results (Figure 8). The optimization of the cumulative energy produced function maximizes the rates achieving the highest value for the cumulative energy produced. However, this is at the expense of the generated NPV. Even though the NPV initially increases faster than the converged solutions with an active BHP penalty, it remains flat after circa 15 years and results in a lower value after 30 years. Contrary to this, the optimization of the NPV function increases both the cumulative energy produced and the generated NPV compared to the optimized functions with an active BHP penalty. The removal of the BHP penalty allowed both optimization functions to utilize higher rates and therefore resulted in reduced production temperatures at the end of the 30 years of simulation.

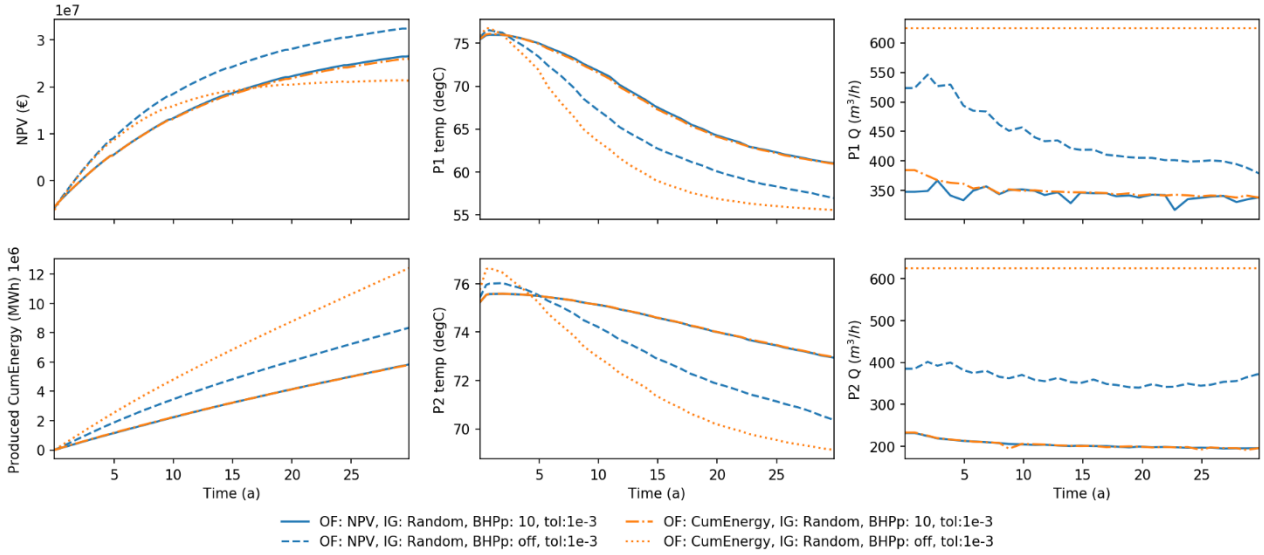

Figure 8. Comparison of the converged solution of the optimization functions of NPV and cumulative produced energy.

3.2 Optimization Framework Performance

The framework is implemented in Python and is able to handle various objective functions and nonlinear constraints. Including both final and preliminary attempts, 65 optimization processes have been completed during this work. With appropriate tuning, the framework demonstrates a significant performance even in the derivative-free optimization regime with the full optimization cycle converging in less than seventeen and a half hours at all times and a mean value of less than five hours (Figure 9).

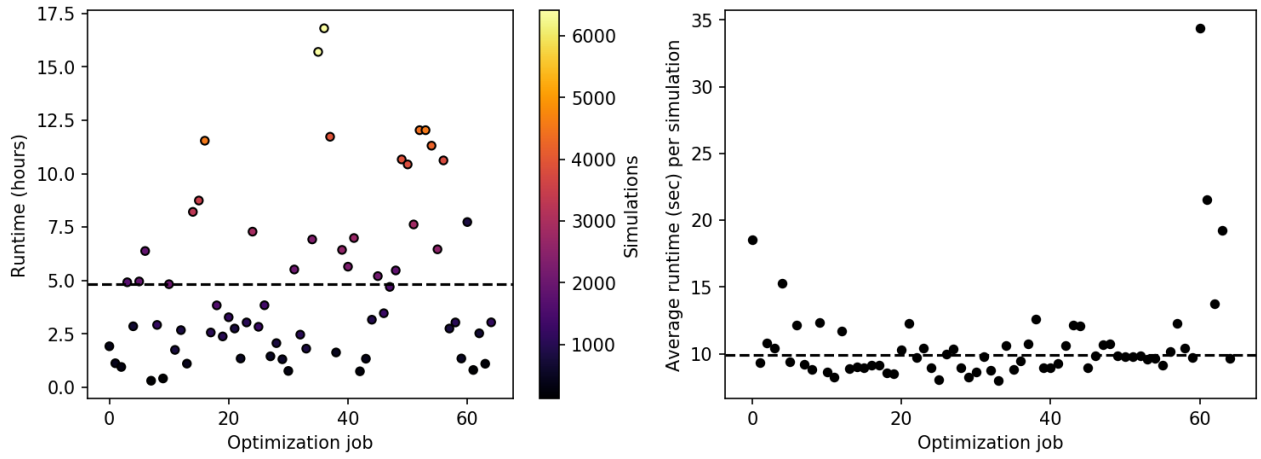

Figure 9. Runtime in hours for each optimization job (left-hand side) and average runtime per simulation (right-hand side). The dashed line marks the mean value.

The performance in each specific optimization depends on the ratio between the amount of function and gradient evaluations, there were 6.779 of the former and 1.782 of the latter in total. Consequently, 113.699 full-scale simulations (i.e., circa 100k cells for 30 year period) have been completed overall. The total computational time taken by the optimization processes was evaluated to 1.129.538 seconds. Neglecting the time spent on the objective function calculations, the average runtimes of a single full-scale simulation amounted to 9.93 seconds (Figure 9).

3.3. Forward simulation comparisons & visualizations

The forward simulation results using the converged rates of the NPV optimization are shown in Figure 10. It is evident that no single doublet is directly connected with a high permeable path between the two wells. However, the P1 well is affected by the cold plume from both injectors. This is consistent with the lower production temperatures of the P1 wells observed before (see sections

3.1.1. Energy production and 3.1.2. NPV). Contrary to this, the P2 well is less affected by the cold water displacement of either injector wells and is able to produce higher temperatures for a longer period of time. The production temperatures are also corroborated by the vertical slices along the E-W axis of the model for each doublet (Figure 11)

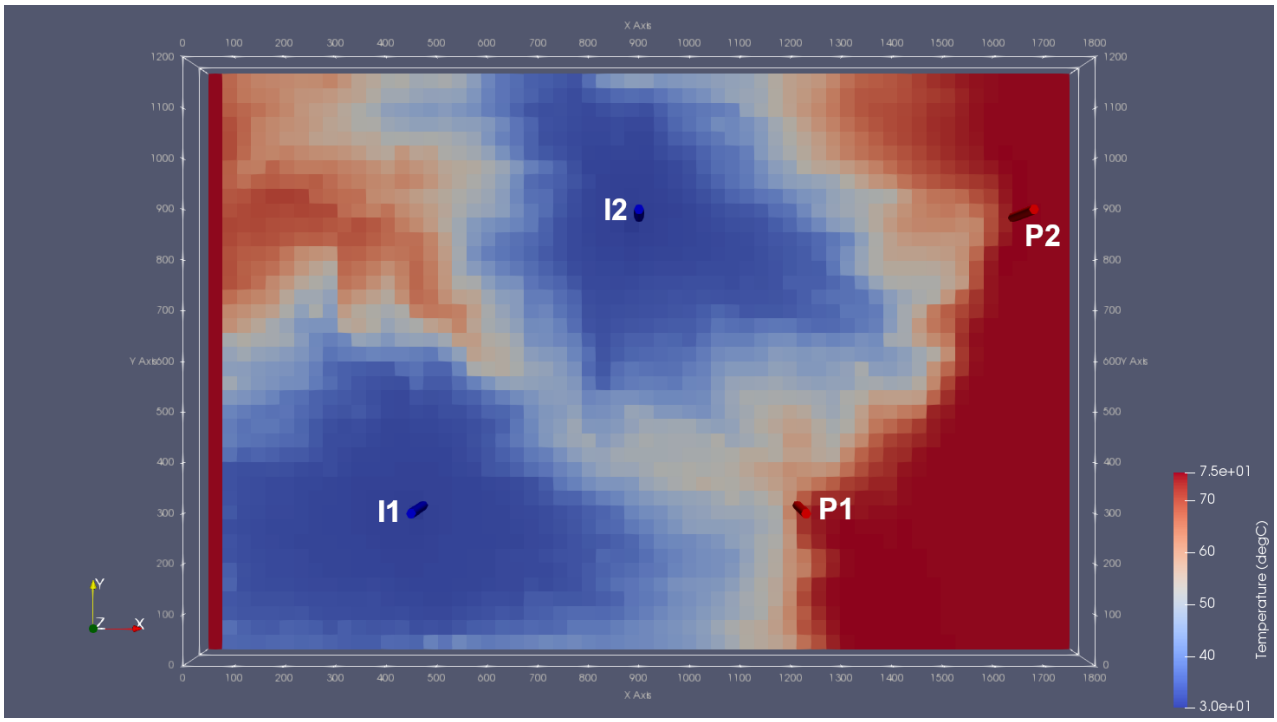

Figure 10. Temperature at middle of the reservoir after the optimized solution of the NPV function, using a tolerance of 1e-3 and an active BHP penalty.

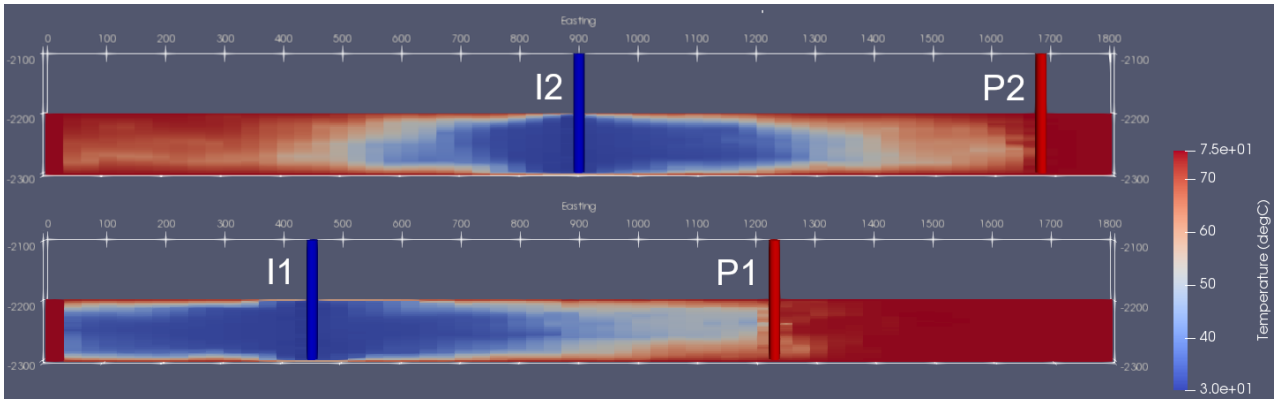

Figure 11. Vertical slices along the E-W axis of both doublets

4. DISCUSSION

The results of the optimization highlight the importance the regulator can have to geothermal developments. The implementation of a BHP constraint effectively streamlines the optimization of different objectives, namely cumulative energy produced and generated NPV. Removing the BHP limit diversifies the results of the optimization functions. When the BHP limit is removed, optimization of the NPV yields more balanced results improving on both cumulative energy generated and NPV. This suggest that the use of NPV as the single objective function to optimize for might be the best option.

The combination of the DARTS simulator with the SLSQP optimizer proved to be highly efficient computationally. An additional benefit is that the user can perform the full analysis and implementation through Python code. This enables a centralized control of the whole process and removes the overhead of working with multiple software packages.

In the presented work the model was limited to two doublets with fixed well positions. The inclusion of additional parameters that become available to the optimizer might yield further interesting results. These parameters could include a larger number of wells, the positioning of the wells and possibly the inclusion of faults in the reservoir domain. Despite the high computational performance of the presented framework, additional degrees of freedom to the optimization process might still become challenging. Adjoint based production optimization of larger problems could therefore be a direction to further investigate, as it could significantly accelerate the convergence under increasing degrees of uncertainty (Sarma et al., 2006; Volkov and Voskov, 2016).

5. CONCLUSIONS

In this work a high performance framework for optimization of geothermal systems has been developed that offers significant performance even in the derivative-free optimization regime. Tuned appropriately the framework achieved an average convergence time below 5 hours for the full optimization cycle and an average simulation runtime just below 10 seconds. This benefit will become progressively more important as more uncertainties are included in the optimization processes.

The model used in this study included a heterogeneous reservoir with two doublets. Each doublet had a well spacing of 780 m and the locations of the wells was kept constant throughout the study. The optimizer was allowed to change the well rates between 0.042 m^3/h and 625 m^3/h on a yearly basis. Within each doublet, both wells had the same flow rate at all times. A constraint was added with regards to the maximum injection pressure allowed by a regulating body. The optimization process was repeated from different initial guesses; three different uniform values and one random value. Moreover the tolerance was altered and the constraint on the maximum injection pressure was also removed.

Two different objective functions are optimized, the cumulative produced energy and the generated NPV. Applying regulatory constraint in terms of maximum allowed injection pressure, the converged solutions for both optimizations arrived to almost identical solutions. Removing this constraint resulted in higher cumulative energy produced for both objective functions while the NPV improved further only for the NPV objective function optimization. Therefore, between the two objective functions considered, the NPV function is able to achieve more comprehensive results, improving other aspects of the system as well. In future efforts, a comparison between the objective functions investigated here with additional ones, such as maximizing system lifetime could better illuminate the different options for geothermal field development.

REFERENCES

Akin, S., Kok, M. V., Uraz, I., 2010. Optimization of well placement geothermal reservoirs using artificial intelligence. Comput. Geosci. https://doi.org/10.1016/j.cageo.2009.11.006

Barros, E.G.D., den Hof, P.M.J., Jansen, J.D., 2019. Informed production optimization in hydrocarbon reservoirs. Optim. Eng. https://doi.org/10.1007/s11081-019-09432-7

Chen, B., Fonseca, R.-M., Leeuwenburgh, O., Reynolds, A.C., 2017. Minimizing the Risk in the robust life-cycle production optimization using stochastic simplex approximate gradient. J. Pet. Sci. Eng. 153, 331–344. https://doi.org/10.1016/J.PETROL.2017.04.001

Daniilidis, A., Alpsoy, B., Herber, R., 2017a. Impact of technical and economic uncertainties on the economic performance of a deep geothermal heat system. Renew. Energy 114, 805–816. https://doi.org/10.1016/j.renene.2017.07.090

Daniilidis, A., Nick, H.M., Bruhn, D.F., 2020. Interdependencies between physical, design and operational parameters for direct use geothermal heat in faulted hydrothermal reservoirs. Prep.

Daniilidis, A., Scholten, T., Hooghiem, J., De Persis, C., Herber, R., 2017b. Geochemical implications of production and storage control by coupling a direct-use geothermal system with heat networks. Appl. Energy 204, 254–270. https://doi.org/10.1016/j.apenergy.2017.06.056

DARTS, 2019. Delft Advanced Research Terra Simulator (DARTS) [WWW Document]. URL https://darts-web.github.io/darts-web/

Fonseca, R.M., Leeuwenburgh, O., den Hof, P.M.J., Jansen, J.D., 2014. Ensemble-based hierarchical multi-objective production optimization of smart wells. Comput. Geosci. 18, 449–461. https://doi.org/10.1007/s10596-013-9399-2

Jones, E., Oliphant, T., Peterson, P., Others, 2001. SciPy.org [WWW Document]. SciPy Open source Sci. tools Python2. URL https://www.scipy.org/

Kahrobaei, S., Fonseca, R.M., Willems, C.J.L., Wilschut, F., Van Wees, J.D., 2019. Regional Scale Geothermal Field Development Optimization under Geological Uncertainties. Proc. Eur. Geotherm. Congr. 2019 11–14.

Khait, M., Voskov, D., 2019. Integrated Framework for Modelling of Thermal-Compositional Multiphase Flow in Porous Media. SPE Reserv. Simul. Conf. https://doi.org/10.2118/193932-MS

Khait, M., Voskov, D., 2018. Operator-based linearization for efficient modeling of geothermal processes. Geothermics 74, 7–18. https://doi.org/10.1016/j.geothermics.2018.01.012

Kong, Y., Pang, Z., Shao, H., Kolditz, O., 2017. Optimization of well-doublet placement in geothermal reservoirs using numerical simulation and economic analysis. Environ. Earth Sci. https://doi.org/10.1007/s12665-017-6404-4

Oliphant, T.E., 2006. A guide to NumPy. Trelgol Publishing, USA.

Saeid, S., Al-Khoury, R., Nick, H.M., Hicks, M.A., 2015. A prototype design model for deep low-enthalpy hydrothermal systems. Renew. Energy 77, 408–422. https://doi.org/http://dx.doi.org/10.1016/j.renene.2014.12.018

Sarma, P., Durlofsky, L.J., Aziz, K., Chen, W.H., 2006. Efficient real-time reservoir management using adjoint-based optimal control and model updating. Comput. Geosci. https://doi.org/10.1007/s10596-005-9009-z

Shetty, S., Voskov, D., Bruhn, D., 2018. Numerical Strategy for Uncertainty Quantification in Low Enthalpy Geothermal Projects. PROCEEDINGS, 43rd Work. Geotherm. Reserv. Eng. 1–16.

SodM, TNO-AGE, 2013. Protocol bepaling maximale injectiedrukken bij aardwarmtewinning – versie 2.

TNO, 2018. ThermoGIS v2.0 - Economic model [WWW Document]. ThermoGIS v2.0. URL https://www.thermogis.nl/en/economic-model (accessed 7.2.19).

van Essen, G., Zandvliet, M., Van den Hof, P., Bosgra, O., Jansen, J.-D., 2009. Robust Waterflooding Optimization of Multiple Geological Scenarios. SPE J. 14, 202–210. https://doi.org/10.2118/102913-PA

Volkov, O., Voskov, D. V, 2016. Effect of time stepping strategy on adjoint-based production optimization. Comput. Geosci. 20, 707–722. https://doi.org/10.1007/s10596-015-9528-1

Voskov, D. V., 2017. Operator-based linearization approach for modeling of multiphase multi-component flow in porous media. J. Comput. Phys. 337, 275–288. https://doi.org/10.1016/J.JCP.2017.02.041

Wang, Y., Khait, M., Voskov, D., Saeid, S., Bruhn, D.F., 2019. Benchmark test and sensitivity analysis for Geothermal Applications in the Netherlands, in: PROCEEDINGS, 44th Workshop on Geothermal Reservoir Engineering. pp. 1–11.

Wendorff, A., Botero, E., Alonso, J.J., 2016. Comparing Different Off-the-Shelf Optimizers' Performance in Conceptual Aircraft Design. https://doi.org/10.2514/6.2016-3362

Willems, C.J.L., M. Nick, H., 2019. Towards optimisation of geothermal heat recovery: An example from the West Netherlands Basin. Appl. Energy 247, 582–593. https://doi.org/10.1016/j.apenergy.2019.04.083

Willems, Cees J.L., Nick, H.M., Donselaar, M.E., Weltje, G.J., Bruhn, D.F., 2017a. On the connectivity anisotropy in fluvial Hot Sedimentary Aquifers and its influence on geothermal doublet performance. Geothermics 65, 222–233. https://doi.org/10.1016/j.geothermics.2016.10.002

Willems, C. J. L., Nick, H.M., Goense, T., Bruhn, D.F., 2017. The impact of reduction of doublet well spacing on the Net Present Value and the life time of fluvial Hot Sedimentary Aquifer doublets. Geothermics 68, 54–66. https://doi.org/10.1016/j.geothermics.2017.02.008

Willems, Cees J.L., Nick, H.M., Weltje, G.J., Bruhn, D.F., 2017b. An evaluation of interferences in heat production from low enthalpy geothermal doublets systems. Energy 135, 500–512. https://doi.org/10.1016/j.energy.2017.06.129